veterinary sciences

Article

Depot-Specific Expansion Dynamics of Canine Adipose-Derived Stromal Cells: An Exploratory Within-Donor Comparison

Woosuk Kim [1], Jinjoo Choi [2], Iman Janghorban Esfahani [3], Ji-Woong Shin [4] and Jeong Ik Lee [2,5,6,*]

[1] Department of Veterinary Anatomy, College of Veterinary Medicine, Konkuk University, Seoul 05029, Republic of Korea; wskim0503@konkuk.ac.kr
[2] Department of Bio&Healing Convergence, Konkuk University, Seoul 05029, Republic of Korea; pearl1530@konkuk.ac.kr
[3] R&D Center, Glopex Co., Ltd., A2801, Geum Gang Penterium IX Tower, 27 Dongtancheomdansaneop 1-ro, Hwaseong-si 18469, Republic of Korea; john@glopex.kr
[4] Research Institute, Cellpurics Inc., 1279-19 Seohae-ro, Paltan-myeon, Hwaseong-si 18524, Republic of Korea; jwshin@cellpurics.com
[5] Department of Veterinary Obstetrics and Theriogenology, College of Veterinary Medicine, Konkuk University, Seoul 05029, Republic of Korea
[6] Regenerative Medicine Laboratory, Center for Stem Cell Research, Department of Biomedical Science and Technology, Institute of Biomedical Science and Technology, Konkuk University, Seoul 05029, Republic of Korea
* Correspondence: jeongik@konkuk.ac.kr; Tel.: +82-2-2049-6234

Simple Summary

Fat tissue contains cells that can multiply and develop into several tissue types, making them promising for future treatments in veterinary medicine. However, the location where fat is collected may affect how easily these cells can be grown. We compared cells obtained from four fat deposits in three dogs: beneath the skin of the abdomen, groin, and buttock, and from fat inside the abdomen near the liver. We examined how rapidly the cells multiplied during laboratory culture, how well they continued growing after repeated transfers to fresh dishes, and whether they displayed features associated with stem-like cells. Cells from beneath the abdominal skin generally multiplied fastest and showed the greatest early growth. Cells from internal abdominal fat grew most slowly, despite the relatively large amount of fat available at that site. Cells from all four locations displayed characteristics associated with stem-like cells, while their responses in tests of fat, bone, and cartilage formation varied. These preliminary findings indicate that the location of fat collection can influence cell growth in the laboratory. Choosing a suitable site may improve the efficiency of preparing cells for veterinary research, although further studies are needed before drawing conclusions about treatment outcomes.

Academic Editor: Xueming Zhang

Received: 26 October 2026
Revised: 18 November 2026
Accepted: 26 November 2026
Published: 27 November 2026

Copyright: © 2026 by the authors. Licensee MDPI, Basel, Switzerland. This article is an open access article distributed under the terms and conditions of the Creative Commons Attribution (CC BY) license.

Abstract

Recently, adipose tissue (AT) has garnered popularity in human and veterinary regenerative medicine as an abundant source of stem cells, owing to their easy availability and identification. Advancements in regenerative medicine have identified significant factors influencing the proliferative ability and phenotype of adipose-derived stem cells (ADSCs), which hold tremendous therapeutic potential, simplifying the description of the host profile, source of tissue and location, and culture conditions. We aimed to comprehensively characterize the expansion potential of ADSCs and cellular attributes of adherent cell populations obtained from various AT depots, including the subcutaneous (sc)

and visceral (vs) regions, extracted from three 6-year-old male beagle dogs. A novel finding was that vs tissue-derived adherent cells showed the slowest proliferation rate ($p < 0.05$) and population doubling level from the 2nd to 6th passage compared to the other groups. Qualitative RT-PCR analysis indicated the presence of selected stem-cell-associated transcripts, including CD34, CD90, and CD105, in cells derived from the evaluated adipose tissue depots, whereas CD45 transcripts were not clearly detected in the presented gel images. Colony formation was observed in adherent cell cultures derived from all four anatomical depots. Qualitative staining also revealed variable responses to adipogenic, osteogenic, and chondrogenic induction conditions. These findings provide preliminary evidence of depot-specific differences in the proliferation and expansion capacity of canine adipose-derived stromal cells and emphasize the importance of specifying the anatomical source of adipose tissue.

Keywords: adipose-derived stem cell; canine adipose tissue; mesenchymal stem cells; proliferation; surface marker

1. Introduction

Adipose tissue (AT), also known as fat tissue, is rich in adipose-derived stem cells (ADSCs), which have the potential to differentiate into multiple cell types, promote tissue repair, and modulate the immune response. ADSCs have promising desirable characteristics and applications in tissue regeneration. The therapeutic potential of ADSCs lies in their ability to secrete certain beneficial molecules and self-renew, making them promising candidates to treat genetic diseases and for use in reconstruction procedures and cosmetic surgery, where the regeneration and repair of tissues are central to achieving positive outcomes [1–4]. Nevertheless, only a few ADSC products have been approved for clinical application, which is beset by several hurdles [5].

Initially, the most common source of mesenchymal stem cells (MSCs) was the bone marrow (bone marrow-derived stem cells) [6,7]. However, Zuk et al. [8] described isolation of ADSCs from AT. Adipose tissue has been reported to provide relatively high yields of culture-expandable mesenchymal stromal cells compared with bone marrow, although cell yields depend on the isolation and culture conditions [9,10]. In a comparative study involving canine tissues, Chung et al. reported mean cell yields after 6–8 days of primary culture (P0) of $(4.2 \pm 1.7) \times 10^5$ cells/g of adipose tissue and $(1.2 \pm 0.2) \times 10^5$ cells/mL of bone marrow aspirate, respectively [11]. ADSCs derived from humans or mice can also be reprogrammed into induced pluripotent stem cells [3,5]. In addition, the methods to extract ADSCs are less invasive and conserve their undifferentiated status during culture passages [12]. ADSCs have multidirectional differentiation potential; in addition to their osteogenic, chondrogenic, and adipogenic differentiation potential, they are also capable of differentiating into hepatocytes, endothelial cells, smooth muscle cells, skeletal muscle cells, myocardial cells, and pancreatic acinar-like cells [13,14]. These characteristics have encouraged the investigation of ADSCs as a potential cell source for regenerative medicine applications, including tissue engineering and tissue repair [12–14].

Several factors, including donor age, tissue type (brown or white), anatomical location in the host organism, type of surgical procedure, exposure to different environmental conditions, and different culture conditions, may affect the rate of proliferation and potential of differentiation [12]. Previous studies have demonstrated that canine adipose-derived stromal cells possess multilineage differentiation potential, including adipogenic, chondrogenic, and osteogenic differentiation [15]. Studies have reported that canine ADSCs have a faster proliferation rate and a higher proportion of colony-forming cells and

are an ideal source for stem cell transplantation compared to BMSCs [16,17]. Studies using human adipose tissue have also demonstrated depot-dependent differences in the biological characteristics of adipose-derived stromal cells. For example, Baglioni et al. reported that cells derived from subcutaneous adipose tissue exhibited higher proliferation rates and adipogenic differentiation potential than those derived from visceral adipose tissue [9].

According to a PubMed survey of in vivo research that included preclinical experiments and clinical trials, the majority focused on human patients, with fewer veterinary clinical trials [18]. The common sources of ADSCs include subcutaneous (sc), visceral (vs), and infrapatellar fat pads [18–21]. ADSCs are derived from the stromal vascular fraction (SVF), which is a heterogeneous population comprising endothelial cells, pericytes, and immune cells. This perivascular extracellular matrix holds vast therapeutic potential for applications in regenerative medicine and wound healing aimed at the functional restoration of tissues damaged by injury or chronic disease [4]. AT is harvested using microinvasive methods such as Coleman liposuction or lipectomy [22]. The cells from the AT are concentrated and resuspended to obtain the SVF after a combination of mechanical emulsification, enzymatic digestion with collagenase, and centrifugation [5,22]. The complex composition of the SVF contributes to its regenerative abilities as it fosters a microenvironment conducive to tissue repair and regeneration.

Studies comparing the different characteristics of ADSCs derived from different anatomical sites in both humans and animal models have been performed [14,17,23]. Over the past decade, sc fat has emerged as an ideal source of stromal stem cells to produce tissue for use in regenerative medicine [4,5]. The sc abdominal AT is less susceptible to apoptotic stimuli because of its adequate blood supply, which is essential for cell survival [24,25].

Vs ATs are a hormonally active component of the body fat located deep within the abdominal cavity around organs such as the liver, intestine, and kidneys. The characteristics and functions of vs ATs are crucial for energy regulation, secretion of hormones, and different metabolic functions. Their main function is to store energy in the form of lipids [26]. Therefore, managing and preventing health risks associated with excessive abdominal fat accumulation is critical [27]. Monitoring and managing vs fat levels are important aspects of promoting overall well-being and preventing health complications [28,29].

The International Society for Cellular Therapy (ISCT) and International Federation for Adipose Therapeutics and Science (IFATS) have played significant roles in advancing the field of AT-based regenerative medicine. In 2013, the ISCT established the criteria and guidelines for identifying and characterizing MSCs, including those derived from AT, ensuring the quality and consistency of research and clinical applications involving ADSCs. Understanding depot-specific characteristics of ADSCs will help enhance therapeutic and regenerative potential, highlighting the need for standardized nomenclature in ADSC-related research.

The primary objective of this article is to determine whether cells that are obtained from different AT depots exhibit stem cell properties. We compared the proliferative potential and expansion capacity of adipose-derived adherent cells that are derived from several AT depots from the canine sources. In addition, the adherent cells were characterized by colony-forming ability, multilineage differentiation potential, and qualitative RT-PCR analysis of selected stem-cell-associated transcripts. Therefore, this study aimed to build upon the existing evidence by comparing ADSCs derived from several AT depots from the canine sources [2,16–18].

2. Materials and Methods

2.1. Tissue Harvesting and Adherent Cell Isolation

Three 6-year-old male beagle dogs were purchased from a commercial laboratory animal supplier (KOATECH Co., Ltd., Pyeongtaek, Republic of Korea) for research purposes. The animals were not privately owned. The dogs had body weights of approximately 15 kg and body condition scores (BCS) ranging from 4 to 5 on a 9-point scale. All experimental procedures, including surgical tissue collection, were conducted in accordance with the protocol approved by the Institutional Animal Care and Use Committee (IACUC) of Konkuk University (Approval No. KU13174). The dogs underwent surgical procedures specifically for adipose tissue collection from four anatomical depots (sc abdominal, sc inguinal, sc gluteal, and vs falciform), rather than for other clinical or surgical purposes. No animals were euthanized for the purpose of adipose tissue collection. The available ATs at 4 sites of interest (sc abdominal, sc inguinal, sc gluteal, and vs falciform) were dissected and weighed, and 3 g from each sample was used for the subsequent experiments. The tissue was carefully washed and treated with 0.1% (*w*/*v*; 1 mg/mL) collagenase type-I (Worthington Biochemical Co., Lakewood, NJ, USA) in Dulbecco's modified Eagle Medium (DMEM/F12) (Gibco, Carlsbad, CA, USA) for 30–45 min in a shaking water bath at 37 °C to disperse the cells and isolate the SVF. The enzymatic reaction was neutralized by the addition of DMEM/F12, fetal bovine serum (FBS) 10%, and antibiotics (antimycotic 10%). The mixture was subsequently centrifuged at 1600 rpm for 20 min. The supernatant was carefully decanted, the pellet was resuspended in culture media, and the sample was centrifuged at 1600 rpm for 5 min. The resulting SVF was collected and resuspended in culture media before seeding on culture plates at a density of 2×10^4 cells/cm^2. Media was changed in the primary culture every 2 days. The adherent cells were trypsinized and harvested after 5 days. Cells collected at passage 0 and passage 1 were suspended in cell banker media (Nippon Zenyaku Kogyo, Fukushima, Japan) and stored at −80 °C.

For the separate assessment of cell recovery following primary culture, viable nucleated SVF cells were cultured for 7 days, after which adherent cells were harvested and counted. The 7-day adherent cell recovery ratio was calculated by dividing the number of adherent cells recovered after 7 days by the total viable nucleated SVF cell count recorded for the corresponding sample. The ratio was expressed as a dimensionless value.

2.2. Culture Characterization

2.2.1. Proliferation Assay, Population Doubling Level, and Colony-Forming Unit Assay

Cell proliferation and population doubling levels (PDLs) were evaluated using a previously described protocol [30] with minor modifications. The morphology and proliferation rates were confirmed using a monolayer cell culture. After the cells reached proper confluency (85–90%), trypsinization and the trypan blue assay (Life Technologies, Gaithersburg, MD, USA) were performed; the cells were counted, and approximately 2×10^3 cells/well were seeded in a 6-well dish (SPL Life Science, Pocheon-si, Gyeonggi-do, South Korea). The media was changed every 48 h to maintain steady growth from 12 to 96 h. The proliferation and morphology of the cells were confirmed using an inverted microscope (Olympus CKX-53; Olympus Optical, Tokyo, Japan).

To evaluate population doubling levels, cells from the first passage were subcultured at a density of 2×10^4 cells per 100-mm culture dish (SPL Life Science) in triplicate. Cell counts were obtained daily for 5 days until the cultures reached confluence. After washing and trypsinization, viable cells were counted manually using the trypan blue exclusion assay. The population doubling level (PDL) was calculated using the following formula:

$$PD\ level = \frac{[log\ (N / Xo)]}{log\ 2}$$

where N represents the final viable cell count and X_0 represents the initial viable cell count. PDL is a dimensionless measure of the number of population doublings occurring during a culture interval. PDLs were evaluated for successive passages, and cumulative population doubling levels (CPDLs) were obtained by summing the PDLs across passages. Experiments were performed in triplicate.

For the colony-forming unit assay, cryopreserved passage 0 (P0) cells were thawed and expanded to passage 1 (P1). The resulting adherent cells were seeded at a density of 2 cells/cm^2 (115 cells per 100-mm culture dish; SPL Life Sciences). After 14 days of culture, the cells were stained with crystal violet (Sigma-Aldrich, St. Louis, MO, USA). Colonies were counted individually, with each colony defined as a cluster containing more than 50 cells. Colony-forming frequency (%) was calculated by dividing the number of colonies formed by the number of cells initially seeded and multiplying by 100.

2.2.2. Multi-Lineage Differentiation Potential Assay

The stored primary cultures were cultured, and after 5 days they were trypsinized after attaining proper confluency. The harvested cells were used for the differentiation assays. Based on preliminary observations of cell proliferation, different seeding densities were used for cells derived from the four anatomical adipose tissue depots. (For sc inguinal, sc gluteal, and vs falciform cells, the seeding rate was 5×10^4 cells/cm^2, whereas for the sc abdominal group, the seeding rate was 2×10^3 cells/cm^2). For adipogenesis, the original medium was changed on day 3 to one containing DMEM-F12 (Gibco), FBS 10% (Hyclone, Logan, UT, USA), Gluta-MAX 1%, antibiotic 1% (Gibco), 3-isobutyl-1-methylxanthine (IBMX), rosiglitazone, dexamethasone, biotin, d-pantothenate, and human insulin. On day 14, the cells were stained with Oil Red O (Sigma-Aldrich).

Osteogenesis and chondrogenesis were induced using similar procedures: approximately 2×10^3 cells/cm^2 were cultured for 3 days to reach 85% confluency using commercial Canine Chondrocytes and Osteoblastic Differentiation Medium (Cell Applications, Inc., San Diego, CA, USA). On day 14 of osteogenesis, the cells were stained using Alizarin Red (Sigma-Aldrich) to detect osteogenesis, whereas the cells were stained with toluidine blue (Sigma-Aldrich) to detect chondrogenesis.

2.2.3. Reverse Transcription-Polymerase Chain Reaction Analysis of Stem-Cell-Associated Transcripts

Total RNA was extracted from adherent cells derived from each adipose tissue depot using TRI Reagent (Molecular Research Center Inc., Cincinnati, OH, USA) according to the manufacturer's instructions. Complementary DNA (cDNA) was synthesized from 1 μg of total RNA using M-MLV reverse transcriptase (Elpis Biotech, Daejeon, Republic of Korea) and random primers (Takara, Tokyo, Japan).

PCR analysis was performed to examine the transcripts of OCT3/4, NANOG, SOX2, CD34, CD45, CD90, and CD105, with GAPDH used as an internal reference. The primer sequences and expected amplicon sizes are summarized in Table 1.

The resulting PCR products were visualized as gel bands for qualitative assessment of transcript detection.

This analysis was performed as an exploratory assessment of selected gene transcripts and was not intended to establish cell-surface protein expression or definitive mesenchymal stromal cell identity.

Table 1. Sequences of PCR primers.

Markers/Gene	Primer Sequence (5′–3′)	Amplification Size (bp)
Pluripotency		
1. OCT3/4	Forward TGACGACAACAAAAATCT Reverse CAGGCATGTGTTCTCCAG	128
2. NANOG	Forward CCTGCATCCTTGCCAATGTC Reverse TCCGGGCTGTCCTGAGTAAG	98
3. Sox2	Forward AACCCCAAGATGCACAACTC Reverse CGGGGCCGGTATTTATAATC	152
MSC markers		
4. CD45	Forward CTCACGCACACAGGCTCGCA Reverse CCCACCCACTGGCACTGCTG	159
5. CD34	Forward GCCTGCTCAGTCTGCTGCCC Reverse TGGTCCCAGGCGTTAGGGTGA	255
6. CD90	Forward CAGAACACCTCATGGCTGCTGT Reverse GGAGAAACCAGACAGAAGCGA	329
7. CD105	Forward GGTTCACTGCATCAACATGG Reverse AAGCTGAAGCGCACATCACC	278

2.3. Statistical Analysis

Statistical analyses were performed using GraphPad Prism 7 (GraphPad Software, San Diego, CA, USA). Three dogs were considered independent biological replicates (n = 3). Because adipose-derived adherent cells were obtained from four anatomical adipose tissue depots within each dog, differences among depots were evaluated using one-way repeated-measures analysis of variance (ANOVA), with individual dogs treated as matched subjects. For the proliferation assay, comparisons among depots were performed at each culture time point. When a significant overall effect was detected, Tukey's multiple comparisons test was applied. Data are expressed as mean ± standard deviation (SD), and statistical significance was set at $p < 0.05$. Given the limited number of biological replicates, the results were interpreted as exploratory.

3. Results

3.1. Sample Collection and Adherent Cell Yield

Adipose tissue (AT) was harvested from three subcutaneous (sc) depots and one visceral (vs) depot. The total amount of AT collected varied among the anatomical depots, as shown in Table 2. Approximately 3 g of adipose tissue from each depot was used for enzymatic digestion and subsequent cell isolation. The vs falciform depot yielded the greatest amount of AT (16.15 g) and the highest number of viable nucleated stromal vascular fraction (SVF) cells per gram of tissue processed (1.21×10^7 cells/g).

To evaluate cell recovery following primary culture, viable nucleated SVF cells were seeded and adherent cells were harvested after 7 days of culture. The 7-day adherent cell recovery ratio was calculated by dividing the number of adherent cells recovered after 7 days by the total viable nucleated SVF cell count recorded for the corresponding sample. The highest recovery ratio was observed in the sc gluteal depot (2.31), followed by the sc abdominal (1.54) and sc inguinal (1.03) depots, whereas the vs falciform depot exhibited the lowest ratio (0.94) (Table 2).

Table 2. Tissue and cell yield from the AT depots.

AT Depot	AT Collected (g)	Viable Nucleated Cells/g	Total Viable Nucleated SVF Cells	Adherent Cells Recovered After 7 Days	7-Day Adherent Cell Recovery Ratio
sc abdominal	4.29	4.44×10^6	1.35×10^7	2.08×10^7	1.54
sc inguinal	10.98	9.77×10^6	2.99×10^7	3.07×10^7	1.03
sc gluteal	4.66	2.66×10^6	8.10×10^6	1.87×10^7	2.31
vs falciform	16.15	1.21×10^7	3.66×10^7	3.46×10^7	0.94

Note: AT collected represents the total amount of adipose tissue harvested from each depot. Approximately 3 g of tissue from each depot was processed for cell isolation. Viable nucleated cells per gram were calculated using the weight of adipose tissue processed. The primary-culture recovery ratio was calculated by dividing the number of adherent cells recovered after primary culture by the total viable nucleated SVF cell count reported for the corresponding sample. Recovery ratios were calculated using the original, unrounded cell counts and are expressed as dimensionless values.

3.2. Morphology, Proliferation Curve, and Cell Growth

The adherent cells derived from all four adipose tissue depots exhibited predominantly fibroblast-like morphology, with no obvious morphological differences among the groups at the examined time point (Figure 1).

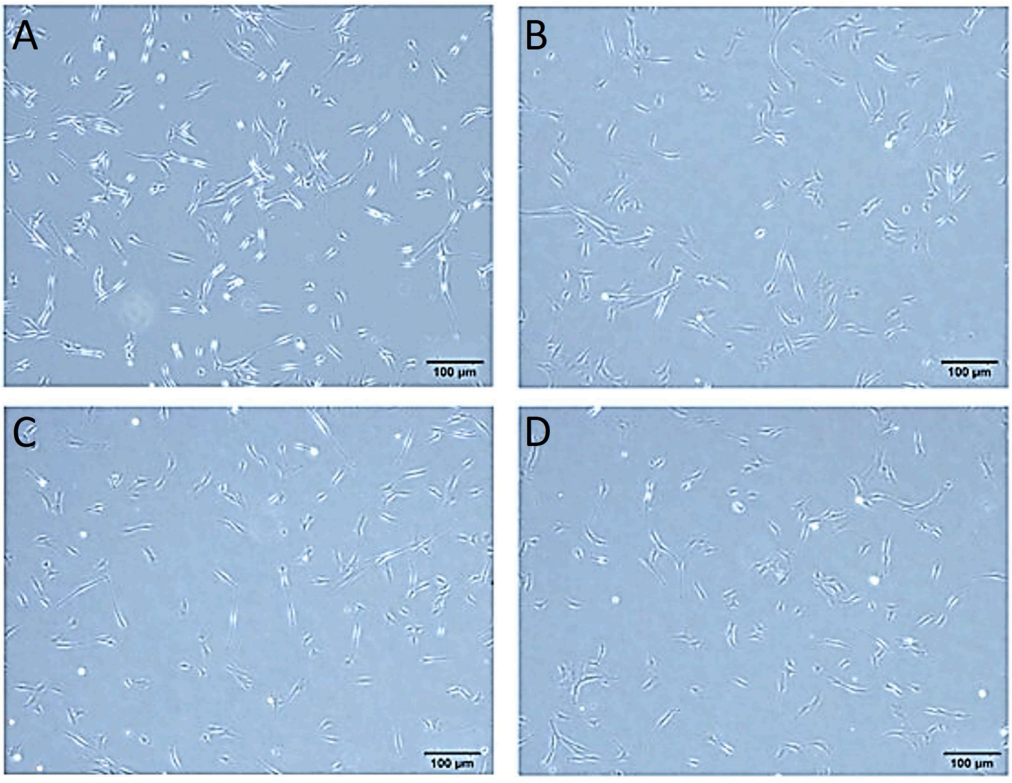


Figure 1. Morphological characteristics of adipose-derived adherent cells from four anatomical adipose tissue depots. Representative images of unstained, plastic-adherent cells obtained on day 3 of the cell proliferation assay. (**A**) sc abdominal, (**B**) sc inguinal, (**C**) sc gluteal, and (**D**) vs falciform adipose tissue-derived cells. The cells exhibited predominantly fibroblast-like morphology.

Cell proliferation was evaluated based on cell counts obtained during 12 days of culture. As shown in Figure 2, the sc abdominal group generally exhibited the highest cell counts, followed by the sc inguinal group, whereas the vs falciform group showed the

lowest cell counts during the later culture period. Specifically, on day 5, the sc abdominal group exhibited the highest cell count, followed by the sc inguinal group. On day 7, the sc inguinal group showed higher cell counts than the sc gluteal and vs falciform groups, and this pattern was also observed on day 8. On day 9, the sc gluteal group exhibited a higher cell count than the vs falciform group. During the later observation period (days 9, 10, and 12), the sc abdominal group maintained the highest cell counts, whereas the vs falciform group showed the lowest cell counts.

To further illustrate the cell growth patterns, the proliferation data presented in Figure 2 were replotted on a semilogarithmic scale (Figure 3). The sc abdominal group showed the most pronounced increase in cell counts, followed by the sc inguinal group, whereas the vs falciform group exhibited the slowest increase. Toward the end of the observation period, cell counts in the sc gluteal and vs falciform groups tended to level off, while those in the sc abdominal and sc inguinal groups continued to increase through day 12.

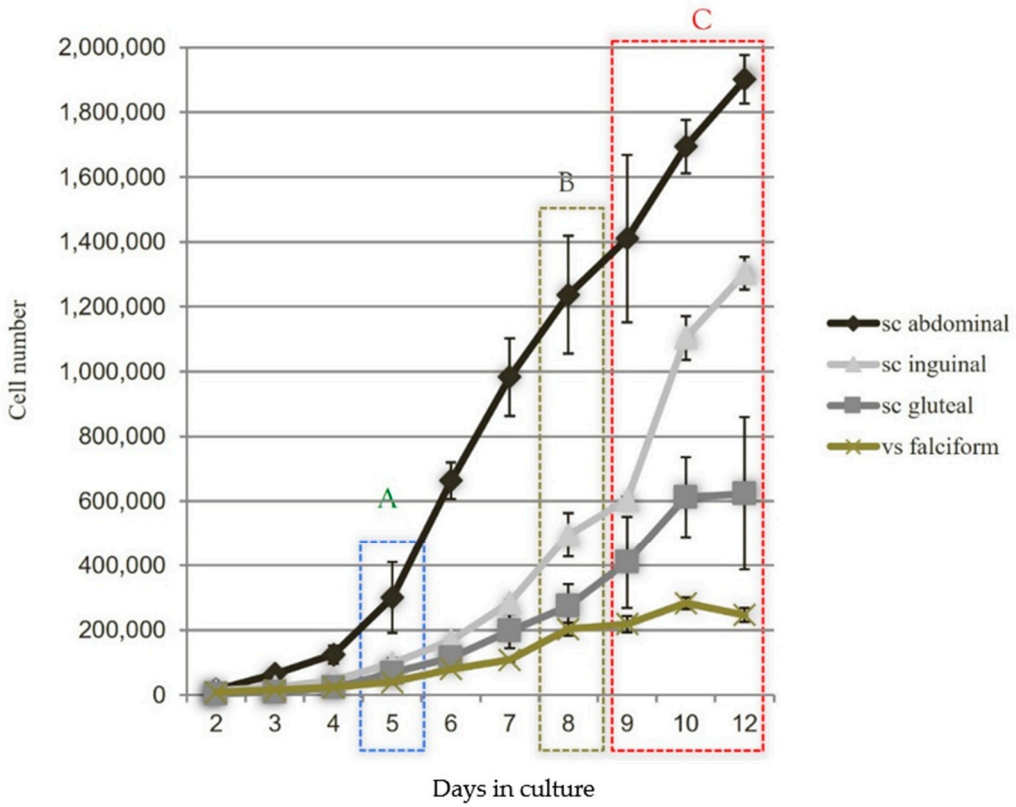


Figure 2. Proliferation curves of adherent cells derived from four anatomical adipose tissue depots during 12 days of culture. The dashed rectangles highlight selected observation points and periods: (A) day 5, when the sc abdominal group exhibited the highest cell count; (B) day 8, when the sc inguinal group showed higher cell counts than the sc gluteal and vs falciform groups; and (C) days 9, 10, and 12, when the sc abdominal group maintained the highest cell counts, whereas the vs falciform group showed the lowest cell counts.

3.3. Total Viable Cell Counts and Population Doubling Level

Our results showed no significant differences in the cell count at different cell passages among the groups, except for the sc inguinal and vs falciform groups (Figure 4). As shown in Figure 4, the sc abdominal group exhibited the highest mean viable cell counts at passages 2 and 3. However, this pattern was not maintained at passage 5, when the sc inguinal and sc gluteal groups showed higher mean cell counts than the sc abdominal group. The vs falciform group exhibited the lowest mean cell count at passage 5. These

observations indicate that the relative cell yields among anatomical depots varied during serial passaging. At passage 6, the sc inguinal group showed a higher cell count than the vs falciform group, but not the sc abdominal group. The vs falciform group had lower cell counts at passages 3, 4, 5, and 6.

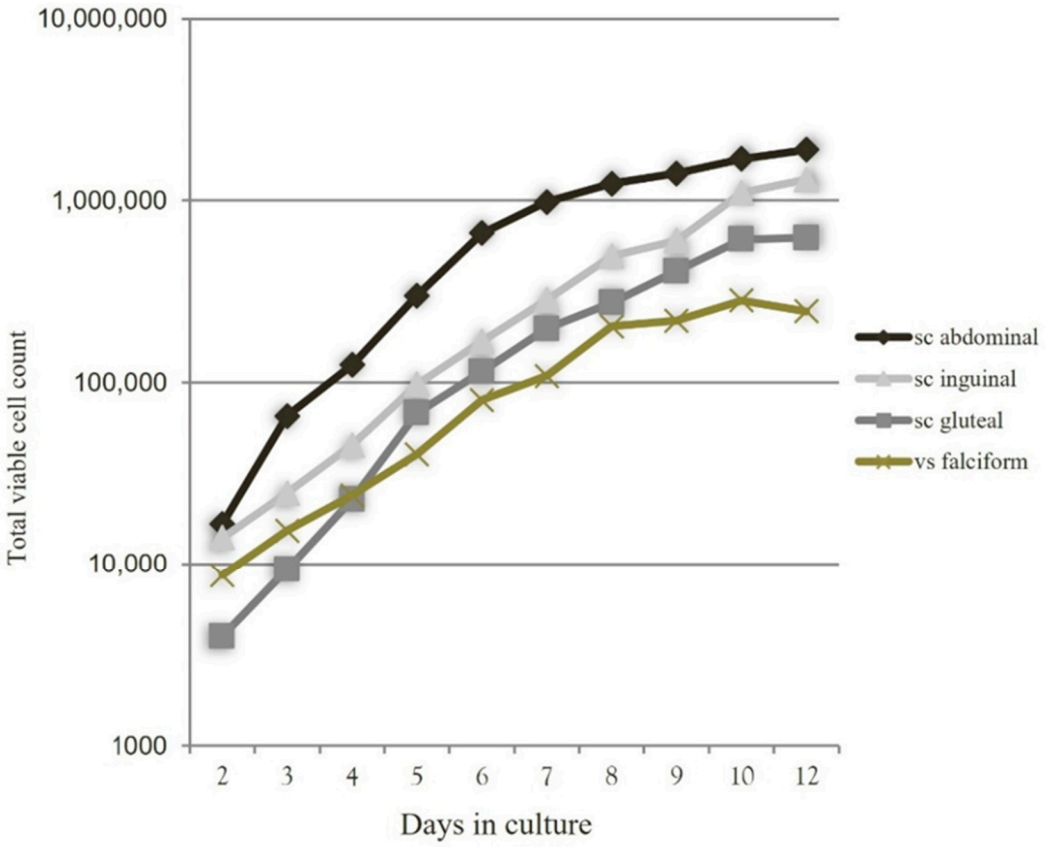


Figure 3. Semilogarithmic growth curves of adherent cells derived from four anatomical adipose tissue depots during 12 days of culture. Cell counts are presented on a logarithmic *y*-axis to illustrate differences in growth patterns among the groups. The sc abdominal and sc inguinal groups showed continued increases in cell counts, whereas the sc gluteal and vs falciform groups exhibited a tendency to plateau toward the end of the observation period.

Population doubling levels (PDLs) were calculated using the formula described in Section 2.2.1 and were compared among the four anatomical adipose tissue depots during serial passaging (Figure 5). Cumulative population doubling levels (CPDLs) were calculated by summing the PDLs obtained at successive passages (Figure 6). As shown in Figure 5, there was no significant difference among the cultures of passage 1 cells except between the sc inguinal and vs falciform groups ($p < 0.05$). Passages 2 and 3 of the sc abdominal group had a higher doubling level, but there were no differences among the groups at passage 4. The change in the doubling level was mainly due to the expansion capacity of the adipose-derived adherent cells derived from various anatomical regions. First, the sc abdominal and inguinal cell numbers were lower at passage 5, which surged at passage 6. In contrast, the vs falciform groups had consistently lower doubling rates throughout all the passages.

Furthermore, population doubling was converted to cumulative population doubling (CPDL) by adding previous levels to the serial passage values. The sc abdominal group increased but remained in line with the sc inguinal cells at the end of the series, while the vs falciform showed slower growth with respect to the CPDL (Figure 6).

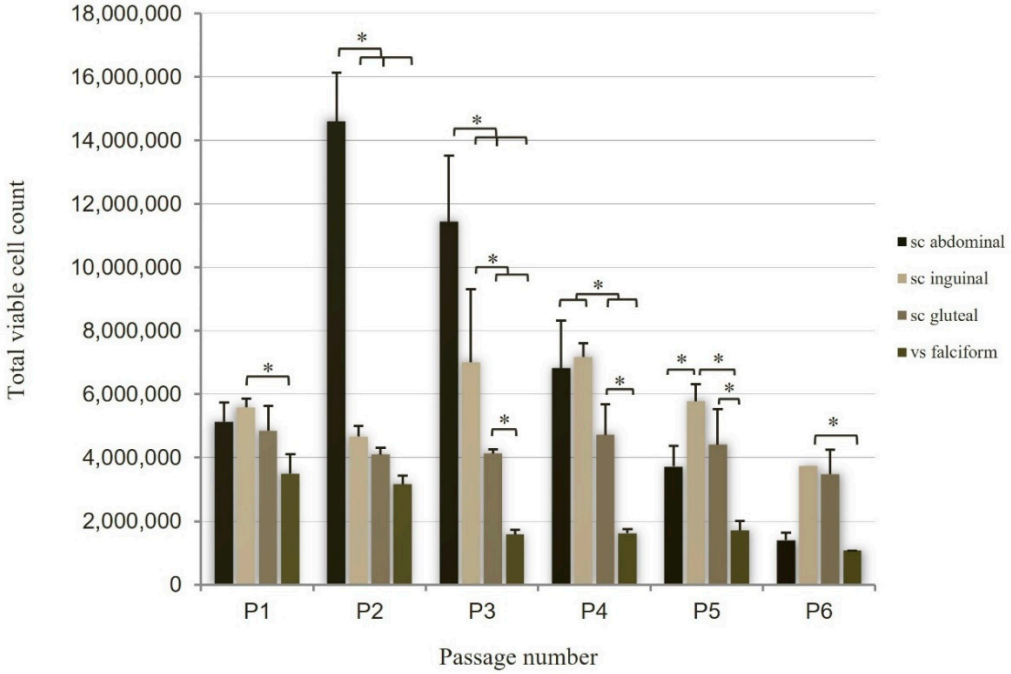


Figure 4. Total viable cell count harvested during serial passage of the adherent cells. The graph shows the total viable counts of adherent cells harvested at the end of each passage from passage 1 to 6 and significant differences among groups (*, $p < 0.05$).

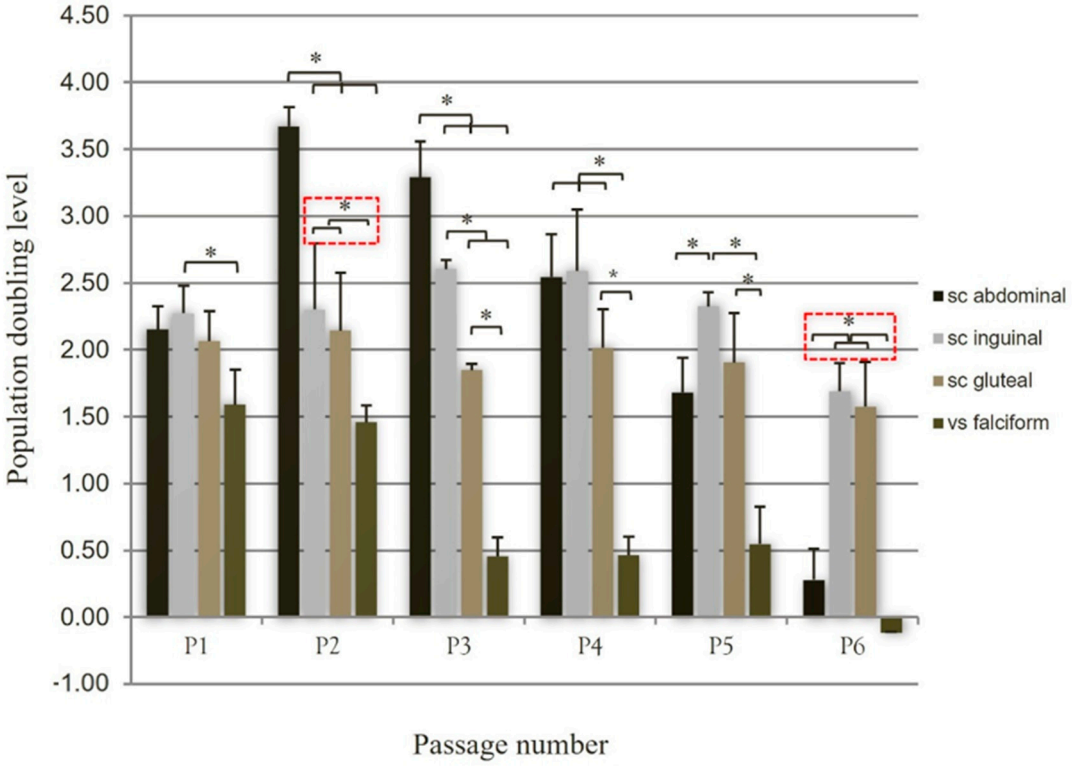


Figure 5. Population doubling levels of adherent cells during serial passaging. Population doubling levels were evaluated from passages 1 to 6 in cells derived from four anatomical adipose tissue depots. The red dashed rectangles highlight selected pairwise comparisons at passages 2 and 6. Brackets and asterisks indicate the comparisons identified as statistically significant (* $p < 0.05$).

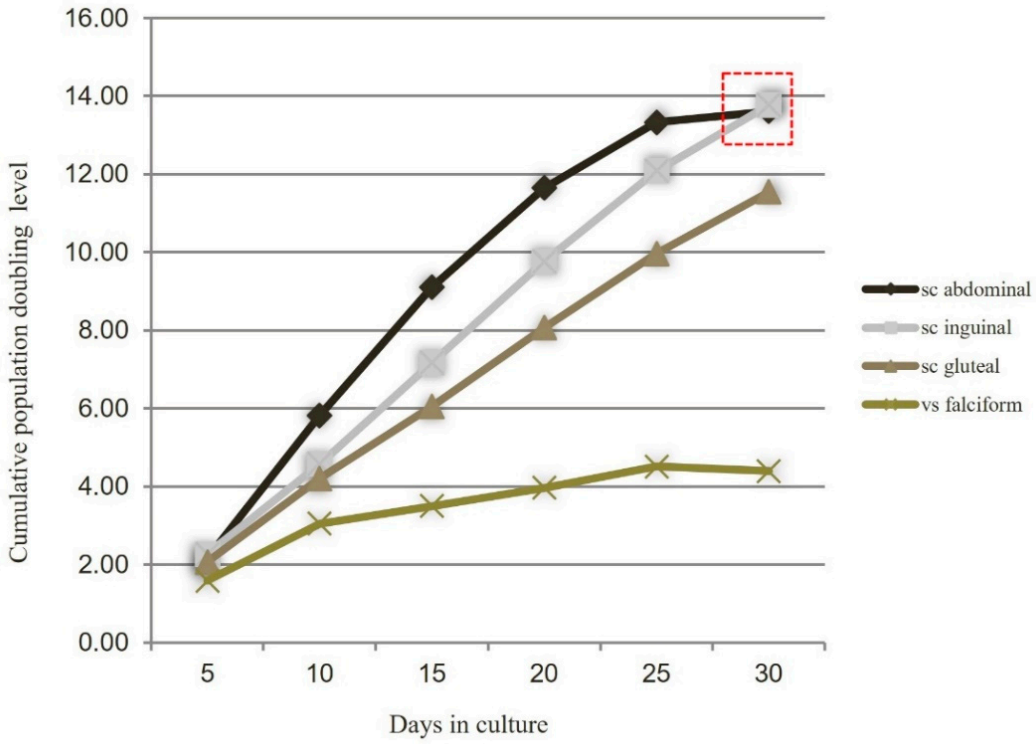


Figure 6. Cumulative population doubling levels of adherent cells during serial passaging. Cumulative population doubling levels were calculated from the population doubling levels obtained during successive passages. The red dashed rectangle highlights the final observation on day 30, when the sc abdominal and sc inguinal groups reached similar cumulative population doubling levels.

3.4. Osteogenic, Chondrogenic, and Adipogenic Differentiation

The differentiation potential of adipose-derived adherent cells was evaluated qualitatively after 14 days of culture under lineage-specific induction conditions. Osteogenic induction was associated with mineralized matrix deposition and positive Alizarin Red staining in the evaluated cultures, with less pronounced staining in the vs falciform group than in the subcutaneous groups (Figure S1).

Under chondrogenic induction conditions, visible deposits of varying sizes were observed in the subcutaneous groups, particularly in the sc abdominal group, whereas comparable changes were not clearly observed in the vs falciform group or the corresponding controls. Representative Toluidine Blue-stained images are provided in Figure S2.

Under adipogenic induction conditions, intracellular lipid droplets and positive Oil Red O staining were observed in representative cultures, whereas comparable changes were not evident in the control images (Figure S3). These observations were qualitative, and differentiation efficiency was not quantified.

3.5. Colony-Forming Unit Assay

Colony-forming ability was assessed in passage 1 adipose-derived adherent cells obtained from four anatomical adipose tissue depots. Following 14 days of culture under low-density seeding conditions, crystal violet-stained colonies were observed in cultures derived from all four depots (Figure S4). These observations provide qualitative evidence of colony formation in the evaluated adherent cell populations. Quantitative comparisons of colony-forming frequency among the anatomical depots were not performed in the present analysis.

3.6. Qualitative RT-PCR Analysis of Stem-Cell-Associated Transcripts

Cells obtained from various adipose tissue (AT) depots were examined by qualitative RT-PCR to assess selected stem-cell-associated transcripts. Bands corresponding to OCT3/4, SOX2, CD34, CD90, and CD105 were observed in the evaluated cultures, whereas NANOG and CD45 bands were not clearly detected in the presented gel images. Differences in band intensity among samples were interpreted qualitatively only and were not considered quantitative differences in gene expression (Figure 7).

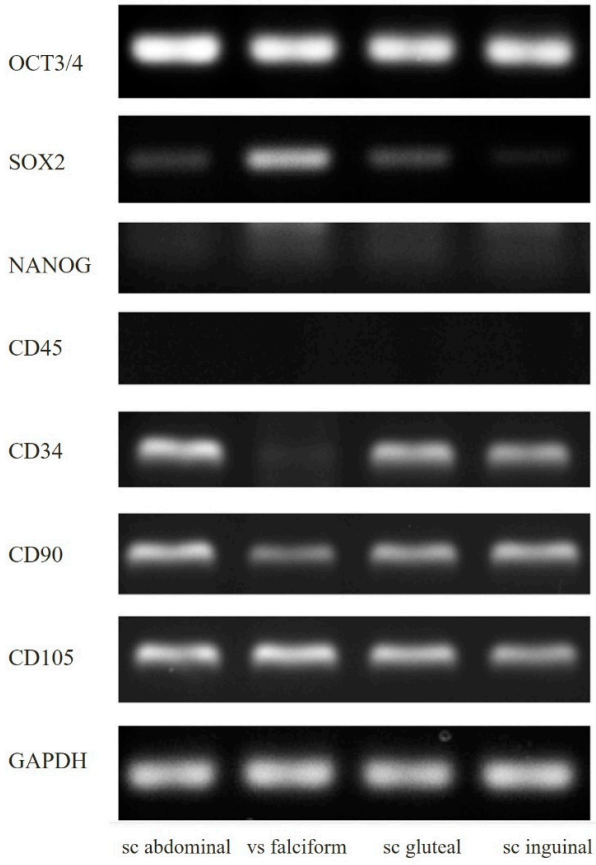


Figure 7. Qualitative RT-PCR analysis of selected stem-cell-associated transcripts in canine adipose-derived stromal cells. Gel images showing PCR amplification products for OCT3/4, SOX2, NANOG, CD45, CD34, CD90, CD105, and GAPDH in adherent cells derived from four anatomical adipose tissue depots: subcutaneous abdominal, visceral falciform, subcutaneous gluteal, and subcutaneous inguinal regions. GAPDH was used as an internal reference. The gel images were assessed qualitatively, and differences in band intensity were not interpreted as quantitative changes in gene expression.

4. Discussion

In the present study, adipose-derived adherent cells were isolated from four anatomical adipose tissue depots in three 6-year-old male laboratory beagle dogs through surgical tissue collection performed specifically for this study. For ADSC isolation and analysis, it is relatively easy to obtain a high amount of AT during surgeries without any significant risk for the tissue donor canine. This makes it easier to establish a bank of cryopreserved ADSCs and MSCs. ADSCs are of great therapeutic potential in humans and in veterinary medicine due to their characteristics related to multipotentiality [13], immunomodulation [31], angiogenesis [32], homing to the site of inflammation [33], and antimicrobial effect

[34]. Domestic animals, which have similar pathologies to humans, can serve as animal models for further research [35].

The availability and characteristics of adipose tissue may depend on the body condition and age of the animal. Previous studies have reported age-related physiological changes in dogs [36], and canine aging does not follow a linear relationship with human aging [37]. In the present study, three 6-year-old male laboratory beagle dogs with comparable body weights and body condition scores were used, thereby limiting variation associated with age, sex, and body condition. Nevertheless, the small number of animals limits the generalizability of these findings.

The cell dose, the type of cells, the method of administration, and the number of deliveries are important features affecting the efficacy of stem cell therapy for a given clinical indication [30,38].

Moreover, the in vitro expansion capacity of adipose-derived adherent cells is an important consideration for obtaining sufficient cell numbers for potential therapeutic applications. In the present study, expansion capacity was evaluated based on changes in viable cell numbers during culture, cell yields at successive passages, and population doubling levels (Figures 2–5). These parameters provide measurable indicators of cellular proliferation and expansion characteristics. However, the time required to achieve a specific therapeutic cell dose was not evaluated in this study.

Furthermore, selecting an appropriate adipose tissue depot requires consideration of both the amount of tissue available and the subsequent recovery and expansion characteristics of the isolated cells. Although the vs falciform depot yielded a greater amount of adipose tissue than the sc inguinal depot (16.15 g vs. 10.98 g; Table 2), greater tissue availability does not necessarily indicate superior in vitro expansion capacity. Previous research has also reported differences in SVF cell yields among canine adipose tissue depots [39]. Manufacturing costs and the number of potential therapeutic doses were not directly evaluated in the present study.

In this study, cell proliferation curves and population doubling levels were analyzed to evaluate the in vitro expansion characteristics of adipose-derived adherent cells from different anatomical depots. The sc abdominal group generally exhibited higher cell counts during the later culture period and a greater increase in cell numbers, as illustrated by the proliferation and semilogarithmic growth curves (Figures 2 and 3).

The colony-forming assay demonstrated that adherent cells derived from all four adipose tissue depots were capable of forming colonies under low-density culture conditions (Figure S4). However, because the colony-forming results were evaluated qualitatively, conclusions regarding differences in colony-forming frequency among anatomical depots cannot be drawn from these observations.

Interestingly, the vs falciform depot yielded the highest number of viable nucleated SVF cells per gram of processed adipose tissue (1.21×10^7 cells/g; Table 2), despite showing generally slower cellular proliferation during subsequent culture than the subcutaneous depots (Figures 2 and 3). In contrast, Astor et al. reported significantly lower viable SVF cell yields per gram of tissue from the falciform region than from the inguinal and thoracic wall regions in dogs [39]. Marx et al. also reported viable SVF cell yields from canine inguinal adipose tissue [40], although differences in donor characteristics and isolation protocols limit direct quantitative comparisons between studies.

Despite its high initial SVF cell yield, the vs falciform depot exhibited the lowest primary-culture recovery ratio (0.94), whereas the sc gluteal depot showed the highest ratio (2.31) (Table 2). Notably, the absolute number of adherent cells recovered after primary culture remained highest in the vs falciform depot. These findings suggest that initial viable nucleated SVF cell yield and subsequent adherent cell recovery represent distinct characteristics of adipose-derived cell preparations. Previous investigations have also

documented differences in the isolation and culture characteristics of canine adipose-derived mesenchymal stromal cells [15]. Nevertheless, the observed differences in recovery ratio cannot be attributed solely to cell attachment, survival, or proliferation without further experimental evaluation.

Serial passaging analyses revealed passage-dependent differences in the expansion characteristics of adipose-derived adherent cells from the four anatomical depots. The sc abdominal group exhibited relatively high viable cell counts and population doubling levels at passages 2 and 3 (Figures 4 and 5). However, this pattern was not consistently maintained during subsequent passages. At passage 5, the sc inguinal and sc gluteal groups exhibited higher mean viable cell counts and population doubling levels than the sc abdominal group. Furthermore, the population doubling level of the sc abdominal group declined markedly at passage 6. Nevertheless, its cumulative population doubling level remained relatively high throughout serial culture and approached that of the sc inguinal group by the final observation (Figure 6). These findings suggest that the expansion characteristics of canine adipose-derived adherent cells may vary according to both anatomical depot and passage number.

Our study also revealed that canine ADSCs exhibit adipogenic, chondrogenic, and osteogenic differentiation potential. Osteogenic differentiation was mostly evident in all cultures, irrespective of the source of isolation. Vs falciform cells showed fewer deposits upon chondrogenic differentiation, while cells derived from sc abdominal AT showed the largest deposits compared to the other groups. All groups exposed to adipogenic media showed a spherical structure, indicating the presence of lipid droplets. These droplets were only lightly stained with Oil Red O . However, Oil Red O staining alone should not be considered definitive evidence of adipogenic differentiation, as nonspecific staining has been reported [41].

It is extremely important to specify the site of tissue sampling and the purpose of using that specific type of tissue for the analysis of the role of ADSCs in regenerative medicine. A review of articles published on PubMed indicated that researchers have explored numerous unique characteristics of ADSCs but did not specify the exact location of tissue sampling [21,41,42–45]. ADSCs, derived from various locations, have different doubling times, proliferation rates, and growth capacities, indicating the importance of specifying the site of origin of the harvested tissues.

Rider et al. reported that 18 of 22 differentially expressed stem-cell marker or maintenance genes showed higher expression in human adipose-derived mesenchymal stromal cells than in bone marrow-derived mesenchymal stromal cells [46]. These included genes associated with Wnt signaling (FRAT1 and FZD1), cell-cycle regulation (FGF2, MYC, CDC42, and CCND2), and stem-cell maintenance (MYST1 and HSPA9B). Their findings also demonstrated the importance of autocrine FGF2 signaling in cellular proliferation. However, these molecular pathways were not examined in the present study, and their potential contributions to the observed differences in expansion characteristics among canine adipose tissue depots remain to be investigated.

Qualitative RT-PCR analysis revealed the presence of selected stem-cell-associated transcripts, including OCT3/4, SOX2, CD34, CD90, and CD105, in cells derived from the examined adipose tissue depots. These findings provide preliminary molecular information regarding the cultured adherent cells.

However, transcript detection by RT-PCR does not necessarily indicate corresponding protein expression or establish the immunophenotypic identity of mesenchymal stromal cells. Flow cytometric immunophenotyping was not performed in the present study, as the RT-PCR analysis was intended only as an exploratory assessment of selected gene transcripts rather than a definitive characterization of cell-surface marker expression. Previous studies and consensus guidelines have emphasized the importance of protein-level

immunophenotypic characterization and species-specific considerations when evaluating adipose-derived stromal cells [47–49]. Furthermore, the present analysis was qualitative, and differences in transcript abundance among adipose tissue depots were not quantitatively evaluated.

Therefore, although the isolated cells exhibited morphological and functional characteristics consistent with adipose-derived stromal cells, comprehensive molecular and immunophenotypic characterization remains necessary. The present findings should be interpreted primarily in terms of cellular proliferation and expansion capacity rather than definitive differences in cellular identity or stemness [47,49].

5. Conclusions

In conclusion, our findings suggest that the proliferation and expansion characteristics of canine adipose-derived adherent cells vary according to their anatomical tissue origin. Cells isolated from different adipose tissue depots exhibited fibroblast-like morphology and variable responses to adipogenic, osteogenic, and chondrogenic differentiation conditions. Qualitative RT-PCR analysis provided additional preliminary molecular information, although the definitive molecular and immunophenotypic identities of these cells were not fully established.

Among the examined depots, cells derived from the subcutaneous abdominal region generally exhibited greater proliferation and early expansion capacity than those from other anatomical sites. However, this advantage was not consistently maintained throughout serial passaging. In contrast, cells derived from the visceral falciform region generally demonstrated slower proliferation and expansion.

These preliminary findings highlight the importance of specifying the anatomical origin of adipose tissue when evaluating canine adipose-derived stromal cells. Further studies involving larger numbers of biological donors and comprehensive cellular characterization are required to confirm these depot-specific differences and determine their relevance to future veterinary regenerative medicine applications.

Supplementary Materials: The following supporting information can be downloaded at https://www.mdpi.com/article/10.3390/vetsci13121295/s1, Figure S1: Osteogenic differentiation of canine adipose-derived adherent cells after 14 days of induction. (A) Representative images showing mineralized matrix deposits in osteogenic induction cultures compared with controls. (B) Alizarin Red staining of adherent cells derived from four adipose tissue depots (sc abdominal, sc inguinal, sc gluteal, and vs falciform) under osteogenic induction and control conditions. The vs falciform group exhibited less pronounced staining than the subcutaneous groups. Figure S2: Chondrogenic differentiation of canine adipose-derived adherent cells after 14 days of induction. (A) Representative images showing visible deposits in chondrogenic induction cultures compared with controls. (B) Toluidine Blue staining of cultures derived from four adipose tissue depots. Visible deposits were observed in the subcutaneous groups, whereas comparable changes were less apparent in the vs falciform group and controls. These observations were evaluated qualitatively. Figure S3: Adipogenic differentiation of canine adipose-derived adherent cells after 14 days of induction. (A) Representative microscopic images showing intracellular lipid droplets in adipogenic induction cultures compared with controls (scale bar = 50 μm). (B) Oil Red O staining showing lipid-containing structures in induced cultures, which were not evident in the corresponding control images (scale bar = 20 μm). Figure S4: Representative colony formation by canine adipose-derived adherent cells from four anatomical adipose tissue depots. Representative images of crystal violet-stained colonies formed by passage 1 adherent cells derived from the sc abdominal, sc inguinal, sc gluteal, and vs falciform depots after 14 days of culture. Cells were seeded at a density of 2 cells/cm^2 (115 cells per 100-mm culture dish). Colonies were defined as clusters containing more than 50 cells. The images are presented for qualitative assessment of colony formation.

https://doi.org/10.3390/vetsci13121295

Author Contributions: Conceptualization, W.K., I.J.E., J.-W.S. and J.I.L.; software, J.C.; data curation, J.C.; writing—original draft preparation, W.K., I.J.E., J.-W.S. and J.I.L.; writing—review and editing, W.K., J.C., I.J.E., J.-W.S. and J.I.L.; visualization, J.C.; supervision, J.I.L. All authors have read and agreed to the published version of the manuscript.

Funding: This work was supported by a National Research Foundation of Korea (NRF) grant funded by the Korean government (MIST) (No. 2022R1F1A1068732).

Institutional Review Board Statement: The animal study protocol was approved by the Institutional Animal Care and Use Committee (IACUC) of Konkuk University (Approval No. KU13174), date 11 February 2014.

Informed Consent Statement: Not applicable. The animals used in this study were purchased from KOATECH Co., Ltd. (Pyeongtaek, Republic of Korea), a commercial laboratory animal supplier, and were not privately owned animals.

Data Availability Statement: The original contributions presented in this study are included in the article/Supplementary Material. Further inquiries can be directed to the corresponding author.

Acknowledgments: The authors would like to express their sincere gratitude to Ernest Balong Jr. for his dedication and valuable contributions to the experimental work underlying this study.

Conflicts of Interest: The authors declare that they have no competing interests.

Abbreviations

The following abbreviations are used in this manuscript:

AT	Adipose Tissue
ADSCs	Adipose-Derived Stem Cells
Sc	Subcutaneous
Vs	visceral
MSCs	Mesenchymal Stem Cells
SVF	Stromal Vascular Fraction
ISCT	The International Society for Cellular Therapy
IFATS	International Federation for Adipose Therapeutics and Science
DMEM/F12	Dulbecco's modified Eagle Medium
FBS	Fetal Bovine Serum
PDL	Population Doubling: Level
PD	Population Doubling
IBMX	3-isobutyl-1-methylxanthine
CPDL	Cumulative Population Doubling
NRF	National Research Foundation of Korea

References

1. Farhana, S.; Kai, Y.C.; Kadir, R.; Sulaiman, W.A.W.; Nordin, N.A.; Nasir, N.A.M. The fate of adipose tissue and adipose-derived stem cells in allograft. *Cell Tissue Res.* **2023**, *394*, 269–292.
2. Dikmen, T.; Özden Akkaya, Ö.; Nawaz, S.; Erdoğan, M. Characterization of bovine bone marrow derived mesenchymal stem cells and immunostaining of differentiated neurospheres. *J. Hell. Vet. Med. Soc.* **2023**, *74*, 5599–5608.
3. Chan, T.-M.; Chen, J.Y.-R.; Ho, L.-I.; Lin, H.-P.; Hsueh, K.-W.; Liu, D.D.; Chen, Y.-H.; Hsieh, A.-C.; Tsai, N.-M.; Hueng, D.-Y. ADSC therapy in neurodegenerative disorders. *Cell Transplant.* **2014**, *23*, 549–557.
4. Vindigni, V.; Giatsidis, G.; Reho, F.; Dalla Venezia, E.; Mammana, M.; Franco, B. Adipose derived stem cells: Current state of the art and prospective role in regenerative medicine and tissue engineering. In *Regenerative Medicine and Tissue Engineering*; IntechOpen: London, UK, 2013.
5. Yuan, X.; Li, L.; Liu, H.; Luo, J.; Zhao, Y.; Pan, C.; Zhang, X.; Chen, Y.; Gou, M. Strategies for improving adipose-derived stem cells for tissue regeneration. *Burn. Trauma* **2022**, *10*, tkac028. https://doi.org/10.1093/burnst/tkac028.

6. Zhang, R.; Ma, J.; Han, J.; Zhang, W.; Ma, J. Mesenchymal stem cell related therapies for cartilage lesions and osteoarthritis. *Am. J. Transl. Res.* **2019**, *11*, 6275–6289.
7. Strem, B.M.; Hicok, K.C.; Zhu, M.; Wulur, I.; Alfonso, Z.; Schreiber, R.E.; Fraser, J.K.; Hedrick, M.H. Multipotential differentiation of adipose tissue-derived stem cells. *Keio J. Med.* **2005**, *54*, 132–141.
8. Zuk, P.A.; Zhu, M.; Mizuno, H.; Huang, J.; Futrell, J.W.; Katz, A.J.; Benhaim, P.; Lorenz, H.P.; Hedrick, M.H. Multilineage cells from human adipose tissue: Implications for cell-based therapies. *Tissue Eng.* **2001**, *7*, 211–228.
9. Baglioni, S.; Cantini, G.; Poli, G.; Francalanci, M.; Squecco, R.; Di Franco, A.; Borgogni, E.; Frontera, S.; Nesi, G.; Liotta, F. Functional differences in visceral and subcutaneous fat pads originate from differences in the adipose stem cell. *PLoS ONE* **2012**, *7*, e36569.
10. Requicha, J.; Viegas, C.A.; Albuquerque, C.; Azevedo, J.; Reis, R.; Gomes, M.E. Effect of anatomical origin and cell passage number on the stemness and osteogenic differentiation potential of canine adipose-derived stem cells. *Stem Cell Rev. Rep.* **2012**, *8*, 1211–1222.
11. Chung, D.-J.; Hayashi, K.; Toupadakis, C.A.; Wong, A.; Yellowley, C.E. Osteogenic proliferation and differentiation of canine bone marrow and adipose tissue derived mesenchymal stromal cells and the influence of hypoxia. *Res. Vet. Sci.* **2012**, *92*, 66–75.
12. Lee, K.S.; Kang, H.W.; Lee, H.T.; Kim, H.-J.; Kim, C.-L.; Song, J.-Y.; Lee, K.W.; Cha, S.-H. Sequential sub-passage decreases the differentiation potential of canine adipose-derived mesenchymal stem cells. *Res. Vet. Sci.* **2014**, *96*, 267–275.
13. Kang, B.-J.; Ryu, H.-H.; Park, S.S.; Koyama, Y.; Kikuchi, M.; Woo, H.-M.; Kim, W.H.; Kweon, O.-K. Comparing the osteogenic potential of canine mesenchymal stem cells derived from adipose tissues, bone marrow, umbilical cord blood, and Wharton's jelly for treating bone defects. *J. Vet. Sci.* **2012**, *13*, 299–310.
14. Guercio, A.; Di Bella, S.; Casella, S.; Di Marco, P.; Russo, C.; Piccione, G. Canine mesenchymal stem cells (MSC s): Characterization in relation to donor age and adipose tissue-harvesting site. *Cell Biol. Int.* **2013**, *37*, 789–798.
15. Neupane, M.; Chang, C.-C.; Kiupel, M.; Yuzbasiyan-Gurkan, V. Isolation and characterization of canine adipose–derived mesenchymal stem cells. *Tissue Eng. Part A* **2008**, *14*, 1007–1015.
16. Chung, C.-S.; Fujita, N.; Kawahara, N.; Yui, S.; Nam, E.; Nishimura, R. A comparison of neurosphere differentiation potential of canine bone marrow-derived mesenchymal stem cells and adipose-derived mesenchymal stem cells. *J. Vet. Med. Sci.* **2013**, *75*, 879–886.
17. Zhu, X.; Shi, W.; Tai, W.; Liu, F. The comparition of biological characteristics and multilineage differentiation of bone marrow and adipose derived Mesenchymal stem cells. *Cell Tissue Res.* **2012**, *350*, 277–287.
18. Balolong, E.; Lee, S.; Nemeno, J.G.; Lee, J.I. Are they really stem cells? Scrutinizing the identity of cells and the quality of reporting in the use of adipose tissue-derived stem cells. *Stem Cells Int.* **2016**, *2016*, 2302430.
19. Kim, M.; Kim, Y.; Lee, S.; Kuk, M.; Kim, A.Y.; Kim, W.; Kweon, O.-K. Comparison of viability and antioxidant capacity between canine adipose-derived mesenchymal stem cells and heme oxygenase-1-overexpressed cells after freeze-thawing. *J. Vet. Med. Sci.* **2016**, *78*, 619–625.
20. Canapp, S.O., Jr.; Canapp, D.A.; Ibrahim, V.; Carr, B.J.; Cox, C.; Barrett, J.G. The use of adipose-derived progenitor cells and platelet-rich plasma combination for the treatment of supraspinatus tendinopathy in 55 dogs: A retrospective study. *Front. Vet. Sci.* **2016**, *3*, 61.
21. Duan, W.; Lopez, M.J. Effects of cryopreservation on canine multipotent stromal cells from subcutaneous and infrapatellar adipose tissue. *Stem Cell Rev. Rep.* **2016**, *12*, 257–268.
22. Coleman, S.R. Structural fat grafting: More than a permanent filler. *Plast. Reconstr. Surg.* **2006**, *118*, 108S–120S.
23. Yaneselli, K.M.; Kuhl, C.P.; Terraciano, P.B.; de Oliveira, F.S.; Pizzato, S.B.; Pazza, K.; Magrisso, A.B.; Torman, V.; Rial, A.; Moreno, M. Comparison of the characteristics of canine adipose tissue-derived mesenchymal stem cells extracted from different sites and at different passage numbers. *J. Vet. Sci.* **2018**, *19*, 13–20.
24. Naudot, M.; Le Ber, J.; Marcelo, P. TMT-Based Quantitative Proteomics Analysis Reveals Differentially Expressed Proteins between Different Sources of hMSCs. *Int. J. Mol. Sci.* **2023**, *24*, 13544.
25. Gentile, P.; Scioli, M.G.; Bielli, A.; Orlandi, A.; Cervelli, V. Concise Review: The Use of Adipose-Derived Stromal Vascular Fraction Cells and Platelet Rich Plasma in Regenerative Plastic Surgery. *Stem Cells* **2017**, *35*, 117–134. https://doi.org/10.1002/stem.2498.
26. Clinic, C. Visceral Fat. Available online: https://my.clevelandclinic.org/health/diseases/24147-visceral-fat (accessed on 6 September 2023).
27. Walker, G.E.; Marzullo, P.; Ricotti, R.; Bona, G.; Prodam, F. The pathophysiology of abdominal adipose tissue depots in health and disease. *Horm. Mol. Biol. Clin. Investig.* **2014**, *19*, 57–74.

28. Shuster, A.; Patlas, M.; Pinthus, J.; Mourtzakis, M. The clinical importance of visceral adiposity: A critical review of methods for visceral adipose tissue analysis. *Br. J. Radiol.* **2012**, *85*, 1–10.
29. Mittal, B. Subcutaneous adipose tissue & visceral adipose tissue. *Indian J. Med. Res.* **2019**, *149*, 571.
30. Rey, F.; Lesma, E.; Massihnia, D.; Ciusani, E.; Nava, S.; Vasco, C.; Al Haj, G.; Ghilardi, G.; Opocher, E.; Gorio, A. Adipose-derived stem cells from fat tissue of breast cancer microenvironment present altered adipogenic differentiation capabilities. *Stem Cells Int.* **2019**, *2019*, 1480314.
31. Anderson, P.; Souza-Moreira, L.; Morell, M.; Caro, M.; O'Valle, F.; Gonzalez-Rey, E.; Delgado, M. Adipose-derived mesenchymal stromal cells induce immunomodulatory macrophages which protect from experimental colitis and sepsis. *Gut* **2013**, *62*, 1131–1141.
32. Laschke, M.W.; Harder, Y.; Amon, M.; Martin, I.; Farhadi, J.; Ring, A.; Torio-Padron, N.; Schramm, R.; Rücker, M.; Junker, D. Angiogenesis in tissue engineering: Breathing life into constructed tissue substitutes. *Tissue Eng.* **2006**, *12*, 2093–2104.
33. Chen, J.; Li, Y.; Katakowski, M.; Chen, X.; Wang, L.; Lu, D.; Lu, M.; Gautam, S.C.; Chopp, M. Intravenous bone marrow stromal cell therapy reduces apoptosis and promotes endogenous cell proliferation after stroke in female rat. *J. Neurosci. Res.* **2003**, *73*, 778–786.
34. Nijnik, A.; Hancock, R.E. The roles of cathelicidin LL-37 in immune defences and novel clinical applications. *Curr. Opin. Hematol.* **2009**, *16*, 41–47.
35. Volk, S.W.; Theoret, C. Translating stem cell therapies: The role of companion animals in regenerative medicine. *Wound Repair Regen.* **2013**, *21*, 382–394.
36. Lee, S.H.; Kim, J.W.; Lee, B.C.; Oh, H.J. Age-specific variations in hematological and biochemical parameters in middle-and large-sized of dogs. *J. Vet. Sci.* **2020**, *21*, e7.
37. Weir, M.; Llera, R.; Buzhardt, L. How Old is Old? Comparing Dog Age to Human Age. Available online: https://vcahospitals.com/know-your-pet/how-old-is-old-comparing-dog-age-to-human-age (accessed on 26 November 2026).
38. O'Donnell, L.; Turner, L.; Levine, A.D. Part 6: The role of communication in better understanding unproven cellular therapies. In *Reference Guide*; International Society for Cellular Therapy (ISCT): Vancouver, BC, Canada, 2015.
39. Astor, D.E.; Hoelzler, M.G.; Harman, R.; Bastian, R.P. Patient factors influencing the concentration of stromal vascular fraction (SVF) for adipose-derived stromal cell (ASC) therapy in dogs. *Can. J. Vet. Res.* **2013**, *77*, 177–182.
40. Marx, C.; Silveira, M.D.; Selbach, I.; da Silva, A.S.; Braga, L.M.G.d.M.; Camassola, M.; Nardi, N.B. Acupoint injection of autologous stromal vascular fraction and allogeneic adipose-derived stem cells to treat hip dysplasia in dogs. *Stem Cells Int.* **2014**, *2014*, 391274.
41. Kinkel, A.D.; Fernyhough, M.E.; Helterline, D.L.; Vierck, J.L.; Oberg, K.S.; Vance, T.J.; Hausman, G.J.; Hill, R.A.; Dodson, M.V. Oil red-O stains non-adipogenic cells: A precautionary note. *Cytotechnology* **2004**, *46*, 49–56.
42. Harman, R.; Carlson, K.; Gaynor, J.; Gustafson, S.; Dhupa, S.; Clement, K.; Hoelzler, M.; McCarthy, T.; Schwartz, P.; Adams, C. A prospective, randomized, masked, and placebo-controlled efficacy study of intraarticular allogeneic adipose stem cells for the treatment of osteoarthritis in dogs. *Front. Vet. Sci.* **2016**, *3*, 81.
43. Ryu, H.-H.; Lim, J.-H.; Byeon, Y.-E.; Park, J.-R.; Seo, M.-S.; Lee, Y.-W.; Kim, W.H.; Kang, K.-S.; Kweon, O.-K. Functional recovery and neural differentiation after transplantation of allogenic adipose-derived stem cells in a canine model of acute spinal cord injury. *J. Vet. Sci.* **2009**, *10*, 273–284.
44. Ismail, A.; Wagner, S.; Murua Escobar, H.; Willenbrock, S.; Sterenczak, K.; Samy, M.; Abd El-Aal, A.M.; Nolte, I.; Wefstaedt, P. Effects of high-mobility group a protein application on canine adipose-derived mesenchymal stem cells in vitro. *Vet. Med. Int.* **2012**, *2012*, 752083.
45. Kol, A.; Foutouhi, S.; Walker, N.J.; Kong, N.T.; Weimer, B.C.; Borjesson, D.L. Gastrointestinal microbes interact with canine adipose-derived mesenchymal stem cells in vitro and enhance immunomodulatory functions. *Stem Cells Dev.* **2014**, *23*, 1831–1843.
46. Rider, D.A.; Dombrowski, C.; Sawyer, A.A.; Ng, G.H.; Leong, D.; Hutmacher, D.W.; Nurcombe, V.; Cool, S.M. Autocrine fibroblast growth factor 2 increases the multipotentiality of human adipose-derived mesenchymal stem cells. *Stem Cells* **2008**, *26*, 1598–1608.
47. Bourin, P.; Bunnell, B.A.; Casteilla, L.; Dominici, M.; Katz, A.J.; March, K.L.; Redl, H.; Rubin, J.P.; Yoshimura, K.; Gimble, J.M. Stromal cells from the adipose tissue-derived stromal vascular fraction and culture expanded adipose tissue-derived stromal/stem cells: A joint statement of the International Federation for Adipose Therapeutics and Science (IFATS) and the International Society for Cellular Therapy (ISCT). *Cytotherapy* **2013**, *15*, 641–648. https://doi.org/10.1016/j.jcyt.2013.02.006.

48. Screven, R.; Kenyon, E.; Myers, M.J.; Yancy, H.F.; Skasko, M.; Boxer, L.; Bigley, E.C., III; Borjesson, D.L.; Zhu, M. Immunophenotype and gene expression profile of mesenchymal stem cells derived from canine adipose tissue and bone marrow. *Vet. Immunol. Immunopathol.* **2014**, *161*, 21–31. https://doi.org/10.1016/j.vetimm.2014.06.002.
49. Guest, D.J.; Dudhia, J.; Smith, R.K.W.; Roberts, S.J.; Conzemius, M.; Innes, J.F.; Fortier, L.A.; Meeson, R.L. Position Statement: Minimal Criteria for Reporting Veterinary and Animal Medicine Research for Mesenchymal Stromal/Stem Cells in Orthopedic Applications. *Front. Vet. Sci.* **2022**, *9*, 817041. https://doi.org/10.3389/fvets.2022.817041.

Disclaimer/Publisher's Note: The statements, opinions and data contained in all publications are solely those of the individual author(s) and contributor(s) and not of MDPI and/or the editor(s). MDPI and/or the editor(s) disclaim responsibility for any injury to people or property resulting from any ideas, methods, instructions or products referred to in the content.